Supplementary Material for "Temperature-Dependent Far-Infrared Absorption in RDX Single Crystals Using Broadband Time-Domain Terahertz Spectroscopy"

1. Experimental setup

As shown in Fig. S1, the terahertz time-domain spectroscopy (THz-TDS) was employed via a degenerate pump-probe scheme using a Ti:sapphire laser oscillator that produces ~35 fs pulses at the THz emitter position, with a repetition rate of 80 MHz at a center wavelength of 800 nm (~1.55 eV) with a bandwidth of ~40 nm. Detail information about the THz emitter Fe-Pt film can be found in Refs. [1,2]. Lock-in technique was used to collect the signals with the help of an AOM (acousto-optic modulator, not shown in Fig. S1). To obtain the data with high signal-to-noise ratio, each set of data was repeated 12 times to average.

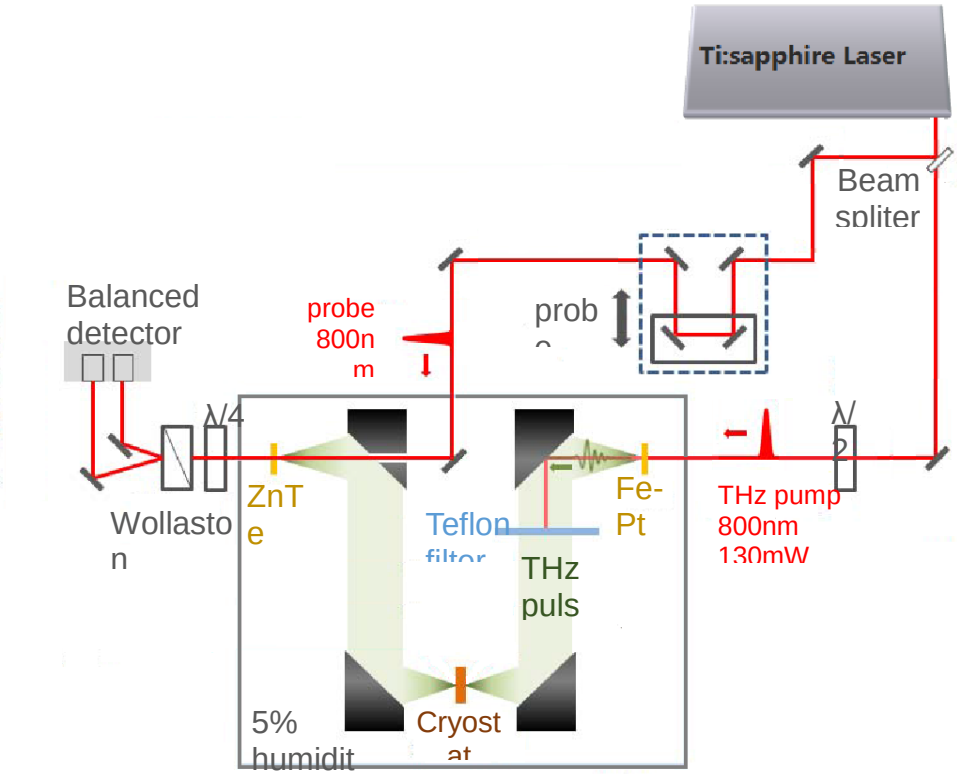

Fig. S1 Schematic diagram of the terahertz time-domain spectroscopy

2. Data processing of FFT

As shown in Figure 1(b) inset of the main text, there is a second THz pulse signal appearing at ~5 ps after the main THz pulse in the time domain even without sample. This arises from the backward and forward reflections of the pump light in the Al_2O_3 substrate of the spintronic THz emitter. Similarly, the third THz pulse signal at ~10 ps arises from the ZnTe crystal. To obtain the frequency domain information, only the data before the second THz pulse (~5.6 ps) are chosen for the fast Fourier Transform (FFT).

The time step of our original data is 20 fs and no interpolation is applied before FFT. To preserve as much signal information as possible, rectangle window is applied during FFT.

The lower frequency limit of our detection is set to ~15 cm^{-1}, due to the low frequency noise up to 7 cm^{-1}. The upper limit is set to 150 cm^{-1}, as the noise floor appears at ~170 cm^{-1}. Noise signals can be seen in the Fig. 1 of the main text.

3. Extracted refractive indices

We employ K-K relation, because it is almost impossible to correctly extracting the phases of the signals in our sample via the reference signals. As we know, the phase is proportional to the sample thickness and the THz frequency. During FFT, the phase is constrained between 0 and 2π. Due to our sample having large thickness compared to those nanoscale thin film, the actual phase values will exceed 2π. Therefore, the obtained values via FFT will have a zigzag-like feature in the frequency domain, where we need to add $2n\pi$ ($n=1,2\cdots$) at the jump points to shift up the related phases and get the correct values. However, the single crystals we used are too thick and can cause strong absorption around those characteristic absorption frequencies. Consequently, large noise is introduced during FFT at those frequencies, and leads to additional false jump points in the phase. Such result is clearly not what we want. Due to the RDX single crystals too fragile, it is impossible to get very thin samples. The above issue cannot be resolved. Therefore, the K-K relation was finally used in our calculations.

The refractive index is calculated using Kramers-Kronig relationship [3]:

$$k(f) = \frac{4\pi}{\lambda_0}\alpha(f)$$

(S1)

$$n(f) = 1 + \frac{2}{\pi} \int_{0, f' \neq f}^{\infty} \frac{f' k(f') - \omega k(f)}{f'^2 - f^2} df'$$

Here, k is the extinction coefficient, f is the frequency (cm^{-1}), λ_0 is the wavelength corresponding to f. Absorption coefficient $\alpha(f)$ is calculated considering only the transmittance component (first term in Eq.1 in the main text). As shown in second formula, the accuracy of refractive index $n(f)$is highly dependent on the frequency range of $\alpha(f)$. Thus, we put our measured $\alpha(f)$ together with high frequency data from Refs.[3][4] to extend the frequency range up to 3700 cm^{-1}. The refractive indices at 5 typical temperatures are shown in Fig. S2.

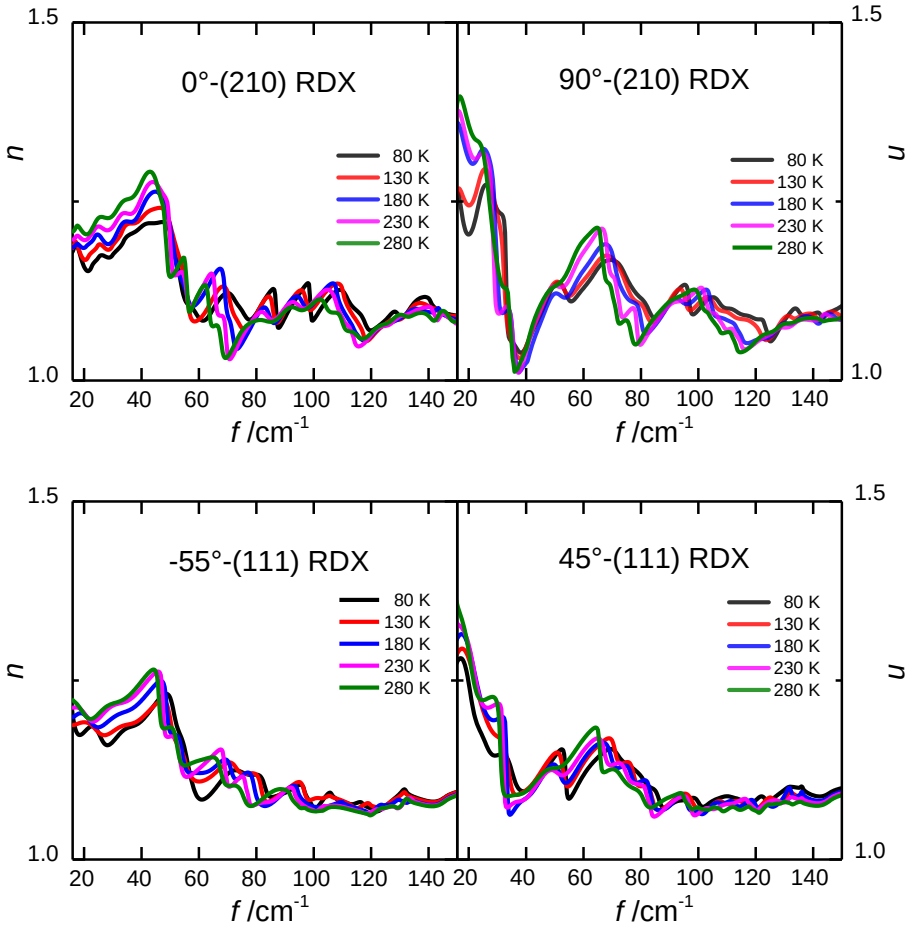

Fig. S2 Temperature-dependent refractive indices of 0°-(210)RDX, 90°-(210)RDX, -55°-(111)RDX, and 45°-(111)RDX. The in-plane orientation is corresponding to Fig. 2 in the main text.

4. Reflection correction term

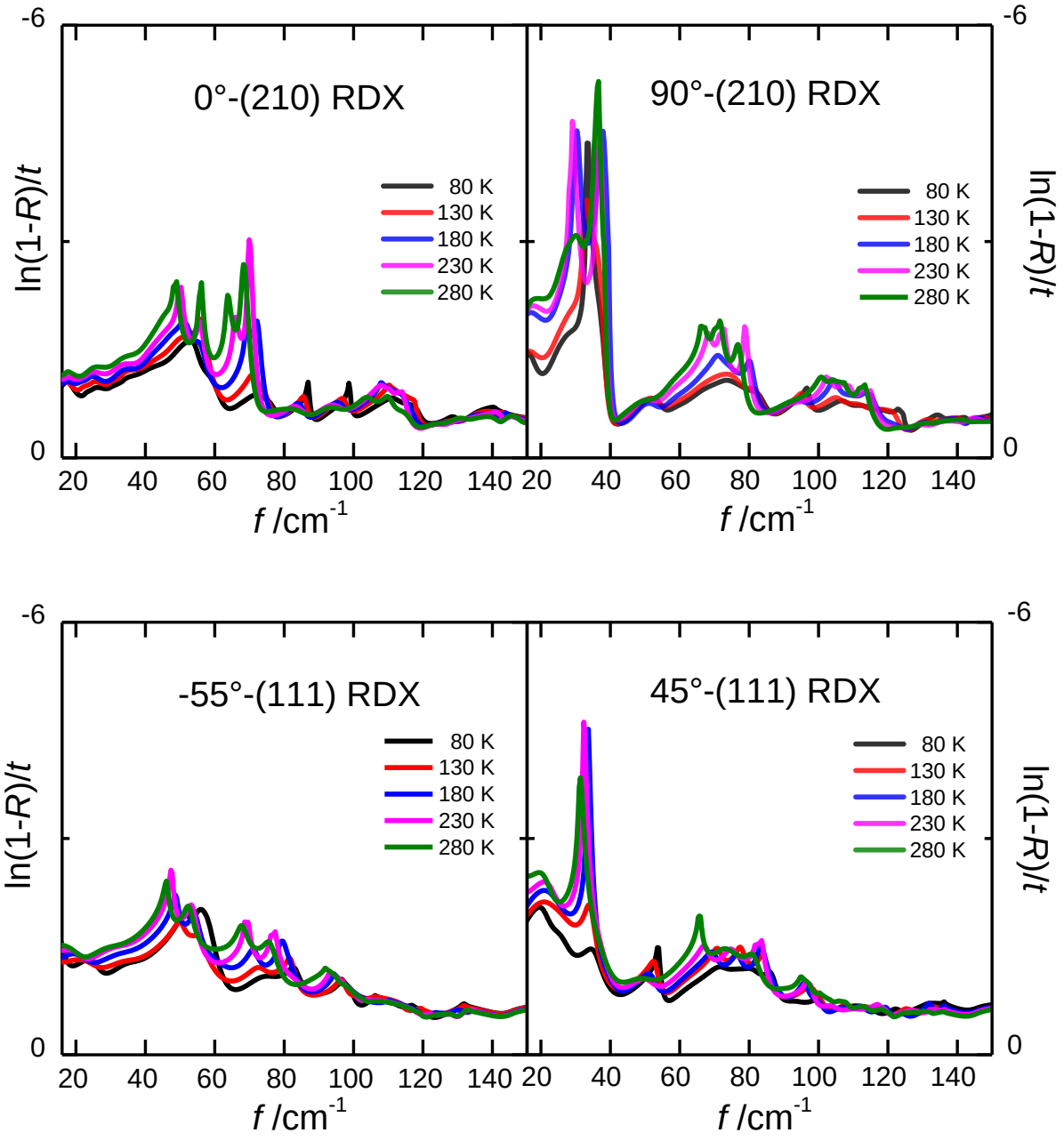

Fig. S3 Temperature-dependent reflection correction term of 0°-(210)RDX, 90°-(210)RDX, -55°-(111)RDX, and 45°-(111)RDX. The in-plane orientation is corresponding to Fig. 2 in text.

Absorption coefficient $\alpha(f)$ is extracted based on:

$$E^2{}_{\text{with sample}}(f) = E^2{}_{\text{without sample}}(f) \cdot (1-R) \cdot \exp(-\alpha t)$$

$$=> \alpha(f) = -\frac{2}{t}\ln\frac{E_{\text{with sample}}}{E_{\text{without sample}}} + \frac{1}{t}\ln(1-R) \tag{S2}$$

As mentioned in the main text, there is a reflection correction term $\frac{1}{t}\ln(1-R)$. Here, reflectivity *R* is given by Fresnel formula:

$$R(f) = \frac{(n-1)^2 + k^2}{(n+1)^2 + k^2} \tag{S3}$$

Results of correction term based on Eq. S1 and S3 are shown in Fig. S3. Considering the magnitude of term $-\frac{2}{t}\ln\frac{E_{\text{with sample}}}{E_{\text{without sample}}}$ (> 100 cm^{-1}), this correction term is proved relative small. The reflection correction is added to $\alpha(f)$ in Figs. 2 and 3 in our text.

5. Dynamic range of absorption

Sometimes the sample is too thick resulting in a discontinuous extrema value for the absorption coefficient. We thus establish the dynamic range as an upper limit of the detectable absorption coefficient. The specific calculation equation is [5]:

$$\alpha_{MAX}(f) = -\frac{2}{t}\ln\frac{E_{\text{noise level}}}{E_{\text{without sample}}(f)} \tag{S4}$$

Here, $\alpha_{MAX}(f)$ is the dynamic range, t is the sample thickness, $E_{\text{without sample}}(f)$ is the THz signal without a sample, and $E_{\text{noise level}}$ is the noise level independent of frequency. It worth noting that the right side of the Eq. S4 is the parameter of the experimental setup and is independent of the sample. The example of dynamic range cutoff is shown in Fig. S4. All the absorption data shown in the main text, also included in Fig. 2 and Fig. 3, take the dynamic range into account. We also redraw Fig. 3 in shape of lines in Fig. S5 at 5 typical temperatures, for the data can be easily assessed. Fitting parameters of phonon modes are listed in Table. S1.

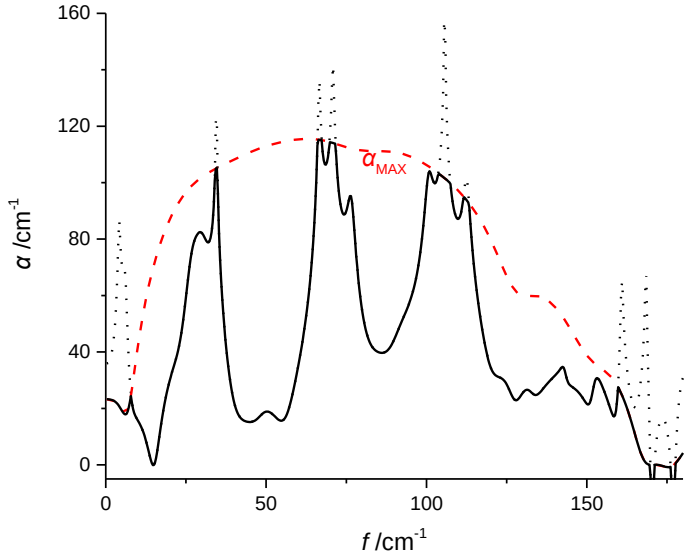

Fig. S4 Temperature-dependent absorption coefficient of (210)-90° RDX at 280 K. Red dashed line is the dynamic range. Black dotted/solid lines are the cut off/ retained parts.

Table. S1 Fitting parameters

Orientation	f_0 (0 K)/ cm^{-1}	$A^{(1)}$/ cm^{-1}
0°-(210)	54.2-59.1	0.39/0.38
	76.5-78.0	1.30/1.00
	88.5	0.67
	100.7	0.91
	115.5-120.6	1.67/0.85
90°-(210)	36.3-37.4	0.48/0.11
	55.1	0.34
	98.4	0.87
	77.7-86.6	1.17/1.07
	109.4-130.3	1.24/3.39
-55°-(111)	53.0-59.8	0.47/0.53
	77.20-87.68	0.94/1.35
	100.6	0.92
45°-(111)	36.8	0.29
	55.1	0.37
	74.9-87.3	0.93/0.70

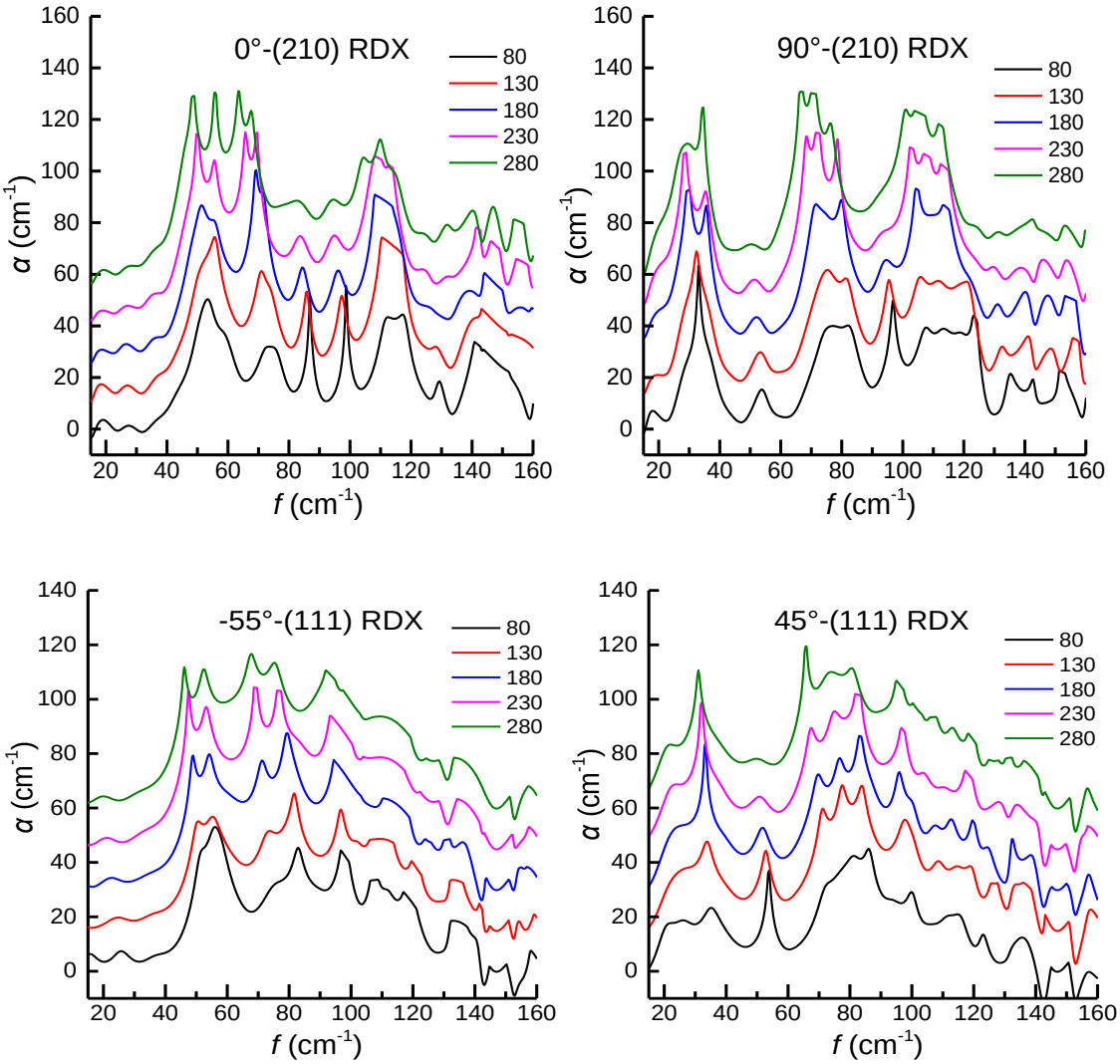

Fig. S5 Temperature-dependent absorption coefficient spectra. The stack constant of the vertical axis α is set to 15 cm^{-1} for a clearer view.

[1] D. W. Yang, J. H. Liang, C. Zhou, L. Sun, R. Zheng, S. N. Luo, Y. Z. Wu and J. Qi, Adv. Optical Mater. 4, 12 (2016).

[2] C. Zhou, Y. P. Liu, Z. Wang, S. J. Ma, M. W. Jia, R. Q. Wu, L. Zhou, W. Zhang, M. K. Liu, Y. Z. Wu, and J. Qi, Phys. Rev. Lett. 121, 086801 (2018).

[3] R. A. Isbell and M. Q. Brewster, Propellants, Explosives, Pyrotechnics 23, 218±224 (1998)

[4] S. W. Sharpe, T. J. Johnson, D.M. Sheen and D.A. Atkinson, Proc. of SPIE Vol. 6378 63780A-1

[5] P. U. Jepsen and B. M. Fischer, Opt. Lett. 30, 1 (2005).